

## Origin of Low-Energy Quadrupole Collectivity in Vibrational Nuclei

C. Walz,<sup>1</sup> H. Fujita,<sup>2,3</sup> A. Krugmann,<sup>1</sup> P. von Neumann-Cosel,<sup>1</sup> N. Pietralla,<sup>1</sup> V. Yu. Ponomarev,<sup>1</sup>  
A. Scheikh-Obeid,<sup>1</sup> and J. Wambach<sup>1,4</sup>

<sup>1</sup>*Institut für Kernphysik, Technische Universität Darmstadt, 64289 Darmstadt, Germany*

<sup>2</sup>*Department of Physics, Osaka University, Toyonaka, Osaka 560-0043, Japan*

<sup>3</sup>*iThemba LABS, Post Office Box 722, Somerset West 7129, South Africa*

<sup>4</sup>*GSI Helmholtzzentrum für Schwerionenforschung, D-64291 Darmstadt, Germany*

(Received 30 November 2010; published 10 February 2011)

The coupling of the giant quadrupole resonance to valence-space configurations is shown to be the origin of the formation of low-lying quadrupole-collective structures in vibrational nuclei with symmetric and mixed-symmetric character with respect to the proton-neutron degree of freedom. For the first time experimental evidence for this picture is obtained from electron- and proton scattering experiments on the nucleus <sup>92</sup>Zr that are sensitive to the relative phase of valence-space amplitudes by quantum interference.

DOI: 10.1103/PhysRevLett.106.062501

PACS numbers: 21.10.Re, 21.60.Ev, 25.40.Ep, 27.60.+j

A general phenomenon of the low-energy structure in heavy atomic nuclei are collective quantum states, in particular, of quadrupole nature. In the context of nuclear structure physics the interacting boson model (IBM) [1] is an example of an effective field theory (EFT), formulated consistently with the symmetries of the intrinsic shapes of the nucleus. It describes the dynamics of collective low-energy nuclear excitations. Effective field theories for relevant low-energy degrees of freedom of complex systems are a concept of fundamental importance in physics with broad applications in many different areas like the Fermi theory of nuclear  $\beta$  decay, Chiral Perturbation theory in strong-interaction physics [2,3], or the BCS theory of superconductivity in condensed matter [4]. The underlying principle is a separation of energy (respectively momentum) scales such that the high-energy degrees of freedom are integrated out leading to a low-energy theory consistent with the symmetries and their breaking pattern. The high-energy sector manifests itself in a set of parameters in the low-energy EFT which have to be determined from experiment. Each EFT is only capable to describe phenomena at a specific (sufficiently low) energy scale.

In the IBM the relevant low-energy degrees of freedom for the description of quadrupole-collectivity are bosons with intrinsic angular momentum  $L = 0$  ( $s$  bosons) or  $L = 2$  ( $d$  bosons). These lead to an effective Hamiltonian whose parameters are adjusted to data. However, a microscopic and quantitative theory for the derivation of these parameters is still missing. Attempts have been made within the valence-shell model [5] with partial success. Such an approach could only be hoped to be successful if the dominant part of the quadrupole collectivity would indeed originate from the valence shell. It is the purpose of this Letter to report new experimental evidence on how the coupling to cross-shell transitions forming the giant quadrupole resonance (GQR) contributes to the formation of low-energy nuclear collectivity. This is achieved by an analysis of transition densities in electromagnetic and

hadronic scattering reactions that enable us for the first time to observe and understand the interference of the valence-shell components of the quadrupole phonon wave functions with those stemming from cross-shell excitations.

To keep the discussion transparent, we study the formation of quadrupole collectivity in the particularly simple case of a nucleus with a low-energy structure that is dominated by one pair of valence particles each for protons and neutrons. An example is the nucleus <sup>92</sup>Zr with 2 neutrons beyond the  $N = 50$  shell closure and 2 protons beyond the  $Z = 38$  subshell closure. The lowest 2-quasiparticle (2QP) states will therefore have  $\pi(1g_{9/2})^2$  and  $\nu(2d_{5/2})^2$  configurations. Because of the residual proton-neutron interaction two different classes of collective excitations appear at low energy in which the amplitudes of the two most important 2QP configurations are coupled in a symmetric or antisymmetric way, respectively. This has been formalized in the proton-neutron version of the IBM [1] where the former are referred to as fully symmetric (FS) and the latter as mixed-symmetry (MS) states [6,7]. In <sup>92</sup>Zr, experimentally identified candidates are the  $2_1^+$  and  $2_2^+$  states [8,9], albeit, with some degree of configurational isospin polarization [9–11].

Experimental evidence for different types of mixed-symmetry states exists like the  $1_{ms}^+$  scissors mode in deformed nuclei [12,13] and the  $2_{ms}^+$  one-phonon state in vibrational nuclei [14]. Signatures of a  $2_{ms}^+$  state are a strong  $M1$  transition to the  $2_{fs}^+$  state with matrix elements  $|\langle 2_{fs}^+ || M1 || 2_{ms}^+ \rangle| \approx 1\mu_N$  and a weakly collective  $E2$  transition to the ground state due to its one-phonon character. The importance of the  $2_{fs}^+$  and  $2_{ms}^+$  phonons as fundamental degrees of freedom of low-energy nuclear structure in vibrational nuclei is highlighted by their capability of forming multiphonon-coupled structures, such as, e.g., the  $[2_{fs}^+ \otimes 2_{ms}^+]$  two-phonon states discovered in the

$N = 52$  isotope  $^{94}\text{Mo}$  [15–18], and confirmed in other nuclides, (see, e.g., [9,19,20]).

In a phenomenological valence-space approach to quadrupole collectivity like the IBM-2 a simplified Hamiltonian can be written as

$$H = \epsilon_{\pi} n_{d\pi} + \epsilon_{\nu} n_{d\nu} + 2\kappa Q_{\pi}^{\chi\pi} Q_{\nu}^{\chi\nu}, \quad (1)$$

where  $\epsilon_{\rho}$  and  $n_{d\rho}$  ( $\rho = \pi, \nu$ ) are the  $d$  boson energies and number operators. The dominant part of the crucial proton-neutron interaction is codified in the third term with  $Q_{\rho}^{\chi\rho}$  being the boson quadrupole operators. An increase of the interaction strength  $\kappa$  will strengthen the mixing of the unperturbed proton and neutron boson states and will finally cause the formation of the collective  $2_{\text{fs}}^{+}$  and  $2_{\text{ms}}^{+}$  states connected by a strong  $M1$  transition as seen in experiment. This parameter needs to be fixed empirically to data. Likewise, the low-energy structure of  $^{92}\text{Zr}$  can be described well within the shell model [8,10], but again parameters (effective charges) have to be introduced as to reproduce quadrupole collectivity.

To shed light on the microscopic origin of the effective coupling strength in the valence shell we consider a different theoretical approach, viz., the quasiparticle-phonon model (QPM) [21]. The QPM starts with interacting particle-hole excitations from which “phonons” are generated by the random-phase approximation (RPA) approach. These form elementary degrees of freedom from which a more general Hamiltonian can be derived which allows for multiphonon states. The QPM covers a sufficiently large single-particle space to satisfy the energy-weighted sum-rules. The QPM approach has proven to account very successfully for the low-energy properties in a large number of vibrational nuclei [22–24]. In the spirit of an interpretation of IBM-2 and shell model as EFTs, the QPM can be viewed as “complete theory” including the high-energy degrees of freedom.

The main properties of the  $2_{\text{fs}}^{+}$  and  $2_{\text{ms}}^{+}$  states of  $^{92}\text{Zr}$  and their transitions are compared in Table I with the QPM results [23], that describe the data remarkably well. The QPM wave functions are dominated by the lowest  $\pi$  and  $\nu$  2QP components, that show the expected in-phase and out-of-phase behavior for the  $2_{\text{fs}}^{+}$  and  $2_{\text{ms}}^{+}$  states. The magnetic moments of these states and the strong  $M1$  transition

TABLE I. Comparison of the QPM results for wave function amplitudes (top) and selected observables of the  $2_{\text{fs}}^{+}$  and  $2_{\text{ms}}^{+}$  states in  $^{92}\text{Zr}$  with the TSM and experiment [9,11].

	Full QPM		TSM		Exp.
	$2_{\text{fs}}^{+}$	$2_{\text{ms}}^{+}$	$2_{\text{fs}}^{+}$	$2_{\text{ms}}^{+}$	
$\nu(2d_{5/2})^2$	0.85	-0.54	0.70	-0.70	...
$\pi(1g_{9/2})^2$	0.36	0.57	0.63	0.70	...
$B(E2: 2_{\text{fs}}^{+} \rightarrow 0_1^{+})$ ( $e^2 \text{fm}^4$ )	145		181		158(15)
$B(E2: 2_{\text{ms}}^{+} \rightarrow 0_1^{+})$ ( $e^2 \text{fm}^4$ )	65		60		84(10)
$B(M1: 2_{\text{ms}}^{+} \rightarrow 2_{\text{fs}}^{+})$ ( $\mu_N^2$ )	0.64		0.86		0.37(4)
$\mu(2_{\text{fs}}^{+})$ ( $\mu_N$ )	-0.22		0.33		-0.18(1)
$\mu(2_{\text{ms}}^{+})$ ( $\mu_N$ )	0.75		0.47		0.76(50)

between them originate almost entirely from the valence-shell configurations as it is shown in Fig. 1. However, the  $B(E2)$  strengths are generated to about 80% from many components beyond the valence shell although their total contribution to the wave function norm is of the order of 1%, only.

The role of the GQR is demonstrated in Fig. 1, which shows the running sums of the  $B(M1)$  and  $B(E2)$  transition strengths as a function of the maximum 2QP energy included in the calculation. The  $M1$  strength saturates at about 6 MeV, i.e., only valence-shell configurations are relevant, while the largest part of the  $E2$  strengths exciting the  $2_{\text{fs}}^{+}$  and  $2_{\text{ms}}^{+}$  phonons is generated by states in the energy region of the GQR around 15–20 MeV.

Apparently, three ingredients are needed to describe the quadrupole-collective one-phonon excitations: the dominant proton and neutron valence-shell components and the GQR. To obtain a qualitative understanding of the mechanism dominating the formation of the quadrupole-collective states within a full-space calculation like the QPM, we thus consider a simple three-state model (TSM) taking into account the lowest neutron and proton 2QP states at energies of 1.917 and 3.172 MeV, respectively, and in addition the GQR located at 11 MeV. As in Landau-Migdal theory [25] the interaction between the GQR and the quasiparticle states can be approximated by a  $\delta$  function

$$V_{\alpha} = g \langle \alpha | \delta(\vec{r} - \vec{r}') | \text{GQR} \rangle = g \int dr r^2 \rho_{\alpha}(r) \rho_{\text{GQR}}(r), \quad (2)$$

where  $\alpha$  refers to the  $\pi$  or  $\nu$  2QP state, respectively. The parameter  $g$  is the interaction strength and  $\rho_{\alpha}$ ,  $\rho_{\text{GQR}}$  stand for the transition densities taken from the QPM calculation. The value for  $g$  is adjusted to reproduce the experimental energy of the  $2_1^{+}$  state of  $^{92}\text{Zr}$ . Finally, the following Hamiltonian,

$$H_{\text{TSM}} = \begin{pmatrix} E_{\text{GQR}} & -V_{\pi} & -V_{\nu} \\ -V_{\pi} & \epsilon_{\pi} & 0 \\ -V_{\nu} & 0 & \epsilon_{\nu} \end{pmatrix}, \quad (3)$$

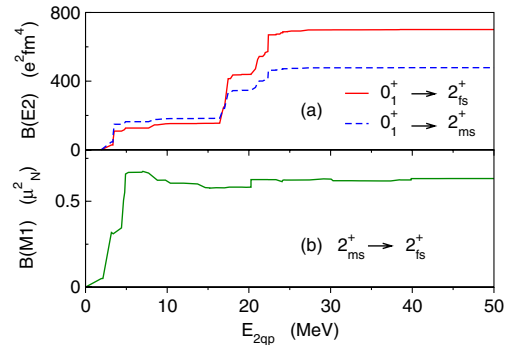


FIG. 1 (color online). Transition strengths as a function of the maximum 2QP energy included in the QPM calculation for (a) ground state excitation of the  $2_{\text{fs}}^{+}$  and  $2_{\text{ms}}^{+}$  states, and (b)  $M1$  transition between both states.

is diagonalized. Here,  $E_{\text{GQR}}$ ,  $\epsilon_\nu$  and  $\epsilon_\pi$  stand for the unperturbed energies. The interaction matrix elements in the valence space are a factor 4 to 8 smaller than those for the GQR and are neglected for simplicity. The results of this simple scheme are confronted with the QPM calculation in Table I. The main properties, i.e., formation of predominantly symmetric and antisymmetric (with negative neutron amplitude due to its lower 2QP energy) one-quadrupole phonon states and  $B(E2)$  and  $B(M1)$  values are well reproduced in this simplified approach except that the model somewhat overestimates the contribution of the proton component to the  $2_{\text{fs}}^+$  state.

Our first result is that the collectivity of the  $2_{\text{fs}}^+$  and  $2_{\text{ms}}^+$  states results predominantly from their coupling to the GQR. The amplitudes of the states forming the GQR in their wave functions are small, but the  $E2$  matrix element  $\langle 0_1^+ || E2 || \text{GQR} \rangle$  is roughly 6 times larger than that of the proton 2QP state, and the  $B(E2)$  strength is mainly produced by the GQR. This effect has previously been recognized [26]. Secondly, the interaction with the GQR not only produces the quadrupole collectivity of the low-lying states but also causes a mixing of the two 2QP states in the valence shell resulting in the formation of symmetric and mixed-symmetric states at low excitation energies.

Can we find experimental evidence for this simple scheme, i.e., is it possible to find a signature for the different interference of the dominant valence-shell components with the high-energy mode as predicted in the TSM? Figure 2 displays the proton and neutron transition densities of the  $2_{\text{fs}}^+$  (top) and  $2_{\text{ms}}^+$  (bottom) states calculated in the full QPM approach. The full transition densities (solid curves) are decomposed in a collective part stemming from the GQR (dotted curves) and the predominant 2QP  $\nu(2d_{5/2})^2$  or  $\pi(1g_{9/2})^2$  contributions (dashed curves). An out-of-phase coupling between the neutron valence-shell contribution and the contribution from the GQR leads to a destructive quantum interference that reduces the neutron transition density at large radii (due to the larger radius of

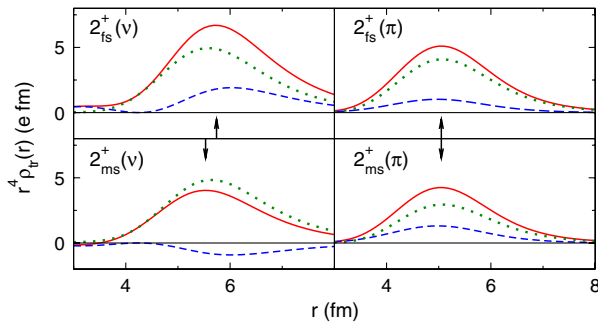


FIG. 2 (color online). Neutron (left-hand side) and proton (right-hand side) transition densities of the  $2_{\text{fs}}^+$  (top) and  $2_{\text{ms}}^+$  (bottom) states in  $^{92}\text{Zr}$  from QPM calculations. The full transition densities (solid lines) are decomposed in parts stemming from the GQR (dotted lines) and from the main 2QP configurations (dashed lines). The arrows indicate the maxima of the corresponding full transition densities.

the  $\nu(2d_{5/2})^2$  orbital) and consequently shifts the maximum of the full neutron transition density to the interior with respect to that one of the  $2_{\text{fs}}^+$  state, as indicated by the arrows in the left-hand side of Fig. 2. This effect reduces the neutron transition radius of the  $2_{\text{ms}}^+$  with respect to the  $2_{\text{fs}}^+$  state. In contrast, the proton transition radius remains essentially unchanged since the  $\pi(1g_{9/2})^2$  part couples in phase to the GQR contribution in both states.

Apparently, two probes with different sensitivity to protons and neutrons are needed to study this quantum interference experimentally which has not been done so far. Electron scattering at low momentum transfer provides a measure of the charge transition radius. An  $(e, e')$  experiment was performed at the high-energy-resolution spectrometer [27] of the Darmstadt superconducting electron linear accelerator (S-DALINAC). An enriched (94.6%) self-supporting  $^{92}\text{Zr}$  target of 9.8 mg/cm<sup>2</sup> areal density was used. Data were taken covering a momentum-transfer range  $q \approx 0.3\text{--}0.6 \text{ fm}^{-1}$  indicating no difference between the charge transition radii of the  $2_{\text{fs}}^+$  and  $2_{\text{ms}}^+$  states within experimental uncertainties (Fig. 3, top). Information about the neutron transition radii can be derived from the proton scattering data of Ref. [28]. At an incident energy of 800 MeV protons interact predominantly via the isoscalar central piece of the effective projectile-nucleus interaction [29]. Clearly, the refraction pattern of the  $(p, p')$  cross section for the  $2_{\text{ms}}^+$  state are shifted to higher  $q$  values as compared to those to the  $2_{\text{fs}}^+$  state (Fig. 3, bottom) corresponding to a smaller transition radius. The combination of both data sets unambiguously demonstrates that the phase of the neutron valence-shell configurations changes its sign between the  $2_{\text{fs}}^+$  and the  $2_{\text{ms}}^+$  state for the first time.

Using the transition densities from Fig. 2, cross sections were calculated in distorted wave Born approximation with the codes DWBA07 [30] for proton scattering and the one

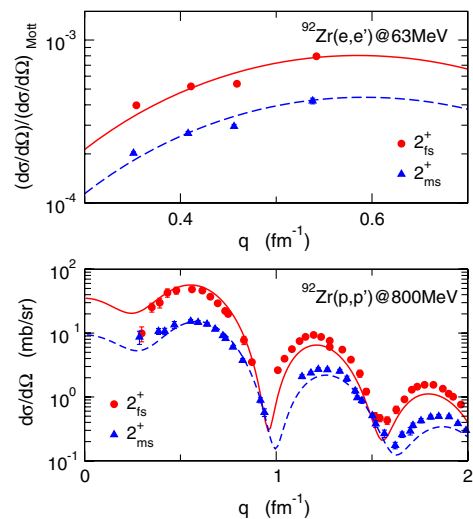


FIG. 3 (color online). Momentum-transfer dependence of the cross sections of the  $2_{\text{fs}}^+$  and  $2_{\text{ms}}^+$  states in electron (top) and proton (bottom) scattering. The data are compared to the QPM calculations.

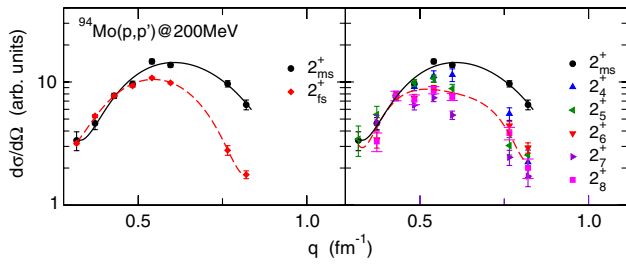


FIG. 4 (color online). Momentum-transfer dependence of the transition to the  $2_{ms}^+$  state in  $^{94}\text{Mo}$  compared to the  $2_{fs}^+$  state (left) and to other low-energy  $2^+$  states (right) measured in the  $(p, p')$  reaction at 200 MeV, normalized to the  $q = 0.43 \text{ fm}^{-1}$  data point. Lines are drawn to guide the eye.

described in Ref. [31] for electron scattering. The  $T$ -matrix parametrization of Franey and Love [29] was used to describe the effective proton-nucleus interaction. The QPM calculation reproduces well both the absolute values of cross sections for both probes and the shift of the refraction pattern to higher  $q$  values for the  $2_{ms}^+$  state in the  $(p, p')$  reaction as displayed in Fig. 3.

This phenomenon is not limited to the nucleus  $^{92}\text{Zr}$ . A smaller transition radius of the  $2_{ms}^+$  state in comparison to the  $2_{fs}^+$  state (and other low-lying  $2^+$  states) is also observed in data sets [18] taken at iThembaLabs and at the S-DALINAC on the isotope  $^{94}\text{Mo}$  (see Fig. 4).

In summary, we presented a simple mechanism to explain the formation of the collective symmetric and mixed-symmetric  $2^+$  states in vibrational nuclei. The proton-neutron quadrupole interaction responsible for the mixing of the valence-space configurations is mediated by their coupling to the GQR, whose contribution dominates the  $E2$  strengths of these states. In contrast, magnetic properties can be understood to a large extent within the scope of effective valence-space models. A combination of proton and electron scattering data provides direct evidence for the interference of high-energy configurations from the GQR with leading valence-space configurations. The data are sensitive to the relative signs of the leading valence-shell configurations with respect to the GQR-contribution and confirm the symmetric and mixed-symmetric nature of the low-energy  $2^+$  one-phonon states. In particular, a flip of phase of the neutron valence configuration between the  $2_{fs}^+$  and the  $2_{ms}^+$  state was observed and is understood as a consequence of the lower neutron than proton  $2\text{QP}$  energy at  $Z = 40$ .

Since typical excitation energies of the low-lying collective states are 1–2 MeV and that of the GQR 10–20 MeV, a clean separation of scales is given, leading to an interpretation of valence-space approaches like the IBM-2 and shell model as EFTs of microscopic models capable to consistently treat valence-shell excitations and giant resonances. While RPA-type models cover sufficient single-particle spaces, they have to truncate on the contribution of many-particle many-hole states to the wave functions. Thus, the construction of effective interactions

in valence-space models remains relevant for a description of low-energy nuclear structure. The present findings highlight the peculiar role played by mixed-symmetry states in such efforts (see, e.g., Ref. [32]) and in our understanding of the formation of nuclear collectivity and of collective phenomena in any strongly coupled multicomponent quantum system.

Fruitful discussions with B. Friman, G. Rainovski, R. V. Jolos, and T. Otsuka are greatly appreciated. This work has been supported by the DFG through grants SFB 634 and NE 679/2-2, and by the South African NRF. We thank the S-DALINAC crew and R. Eichhorn for their commitment in delivering excellent electron beams.

- [1] F. Iachello and A. Arima, *The Interacting Boson Model* (Cambridge University Press, Cambridge, England, 1987).
- [2] S. Weinberg, *Physica (Amsterdam)* **96A**, 327 (1979).
- [3] J. Gasser and H. Leutwyler, *Nucl. Phys. B* **250**, 539 (1985).
- [4] R. Shankar, *Rev. Mod. Phys.* **66**, 129 (1994).
- [5] T. Otsuka, A. Arima, and F. Iachello, *Nucl. Phys. A* **309**, 1 (1978).
- [6] A. Arima *et al.*, *Phys. Lett. B* **66**, 205 (1977).
- [7] F. Iachello, *Phys. Rev. Lett.* **53**, 1427 (1984).
- [8] V. Werner *et al.*, *Phys. Lett. B* **550**, 140 (2002).
- [9] C. Fransen *et al.*, *Phys. Rev. C* **71**, 054304 (2005).
- [10] J. D. Holt *et al.*, *Phys. Rev. C* **76**, 034325 (2007).
- [11] V. Werner *et al.*, *Phys. Rev. C* **78**, 031301 (2008).
- [12] D. Bohle *et al.*, *Phys. Lett. B* **137**, 27 (1984).
- [13] K. Heyde, P. von Neumann-Cosel, and A. Richter, *Rev. Mod. Phys.* **82**, 2365 (2010).
- [14] N. Pietralla, P. von Brentano, and A. Lisetskiy, *Prog. Part. Nucl. Phys.* **60**, 225 (2008).
- [15] N. Pietralla *et al.*, *Phys. Rev. Lett.* **83**, 1303 (1999).
- [16] N. Pietralla *et al.*, *Phys. Rev. Lett.* **84**, 3775 (2000).
- [17] C. Fransen *et al.*, *Phys. Lett. B* **508**, 219 (2001).
- [18] O. Burda *et al.*, *Phys. Rev. Lett.* **99**, 092503 (2007).
- [19] H. Klein *et al.*, *Phys. Rev. C* **65**, 044315 (2002).
- [20] S. Mukhopadhyay *et al.*, *Phys. Rev. C* **78**, 034317 (2008).
- [21] V. Soloviev, *Theory of Atomic Nuclei: Quasiparticles and Phonons* (Institute of Physics Publishing, Bristol, 1992).
- [22] N. Lo Iudice and Ch. Stoyanov, *Phys. Rev. C* **62**, 047302 (2000).
- [23] N. Lo Iudice and Ch. Stoyanov, *Phys. Rev. C* **73**, 037305 (2006).
- [24] N. Lo Iudice, Ch. Stoyanov, and D. Tarpanov, *Phys. Rev. C* **77**, 044310 (2008).
- [25] A. Migdal, *Theory of Finite Fermi Systems* (Interscience Publishers, New York, 1967).
- [26] H. Sagawa *et al.*, *Nucl. Phys. A* **462**, 1 (1987).
- [27] A. W. Lenhardt *et al.*, *Nucl. Instrum. Methods Phys. Res., Sect. A* **562**, 320 (2006).
- [28] F. T. Baker *et al.*, *Nucl. Phys. A* **393**, 283 (1983).
- [29] M. A. Franey and W. G. Love, *Phys. Rev. C* **31**, 488 (1985).
- [30] J. Raynal, code DWBA07 (2007).
- [31] J. Heisenberg and H. P. Blok, *Annu. Rev. Nucl. Part. Sci.* **33**, 569 (1983).
- [32] K. Sieja *et al.*, *Phys. Rev. C* **80**, 054311 (2009).